QED calculations of energy levels of helium-like ions with $5 \leq Z \leq 30$

Vladimir A. Yerokhin,[1] Vojtěch Patkóš,[2] and Krzysztof Pachucki[3]

[1]*Peter the Great St. Petersburg Polytechnic University, Polytekhnicheskaya 29, 195251 St. Petersburg, Russia*
[2]*Faculty of Mathematics and Physics, Charles University, Ke Karlovu 3, 121 16 Prague 2, Czech Republic*
[3]*Faculty of Physics, University of Warsaw, Pasteura 5, 02-093 Warsaw, Poland*

(Dated: August 12, 2022)

A calculation of two-electron QED effects to all orders in the nuclear binding strength parameter $Z\alpha$ is presented for the ground and $n = 2$ excited states of helium-like ions. After subtracting the first terms of the $Z\alpha$ expansion from the all-order results, we identify the higher-order QED effects of order $m\alpha^7$ and higher. Combining the higher-order remainder with the results complete through order $m\alpha^6$ from [V. A. Yerokhin and K. Pachucki, Phys. Rev. A **81**, 022507 (2010)], we obtain the most accurate theoretical predictions for the ground and non-mixing $n = 2$ states of helium-like ions with $Z = 5-30$. For the mixing $2\,^1P_1$ and $2\,^3P_1$ states, we extend the previous calculation by evaluating the higher-order mixing correction and show that it defines the uncertainty of theoretical calculations in the LS coupling for $Z > 10$.

I. INTRODUCTION

Helium and helium-like ions are the simplest few-body atomic systems in nature. They have been extensively studied experimentally, measurements being facilitated by the availability of long-lived metastable ^3S and ^3P states in their spectrum [1]. The simplicity and the long history of experimental studies make helium and helium-like ions a widely used testing ground for different methods of atomic-structure calculations [2, 3]. Alongside with the hydrogen-like atoms, the helium-like ions are the systems for which theoretical predictions are the most accurate [4].

There are two essentially different approaches in *ab initio* QED calculations of atomic energies. The first method, often referred to as the "all-order" approach, starts with the Dirac energies and accounts for the electron-electron interaction by a systematic QED perturbation expansion. In this way one includes all orders in the electron-nucleus binding strength parameter $Z\alpha$ (where Z is the nuclear charge number and α is the fine-structure constant) but expands in the electron-electron interaction parameter $1/Z$. For the high-Z ions the electron correlation effects are small and this approach yields very accurate results [5–7]. For the lower-Z ions, however, the relative contribution of uncalculated higher-order electron-correlation effects grows and the accuracy of the method diminishes. At present the most complete calculations for helium-like ions by this method were reported in Refs. [8–10].

For low-Z systems and especially for the helium atom, the best results are obtained with the method of the nonrelativistic QED (NRQED). The starting point is the few-body Schrödinger equation, which includes the Coulomb electron-electron interaction to all orders. The relativistic and QED effects are accounted for perturbatively, with the expansion parameters α and $Z\alpha$. For the helium atom both parameters are small and the perturbation expansion converges rapidly, yielding highly accurate theoretical predictions [11]. For helium-like ions, however, the parameter $Z\alpha$ becomes larger and the accuracy of the method diminishes, with uncalculated higher-order effects enhanced by high powers of Z (up to Z^9 in the case of fine-structure intervals [12]).

In order to achieve more accurate results, pure NRQED calculations need to be complemented by a separate treatment of higher-order (in $Z\alpha$) effects, based on the all-order calculations. In this way, the two complementary approaches can be merged, yielding an improved accuracy in the region of medium Z, where each of these methods separately encounter difficulties. This "unified" approach was introduced for helium-like ions by Drake in Ref. [13]. It was advanced further in our previous investigation [14], where all effects up to order $m\alpha^6$ were taken into account. Recently, the unified approach was applied to obtain the most accurate predictions for the fine structure of lithium-like ions [15].

The limitation on the accuracy of our previous work on helium-like ions [14] was coming from the fact that the higher-order QED effects were obtained with the inclusion of one-electron effects only (i.e., to the zeroth order in $1/Z$). The identification of the higher-order two-electron QED contributions was not possible at that time, because of insufficient numerical accuracy of the all-order QED calculations.

The goal of the present investigation is to perform a high-precision numerical calculation of the two-electron QED corrections to all orders in $Z\alpha$ and to identify the higher-order $m\alpha^{7+}$ QED contribution to first order in $1/Z$. The higher-order correction obtained in this way is then added to the results of Ref. [14], yielding improved theoretical predictions for ionization energies of helium-like ions.

An additional motivation for the present investigation comes from the observation of a significant discrepancy between theoretical predictions and experimental results for the ionization energies of the triplet $n = 2$ states in the helium atom [16, 17]. In view of this discrepancy, it is important to cross-check the NRQED evaluation of higher-order QED effects [16, 18, 19] against the all-order calculations.

The paper is constructed as follows. Sec. II presents a set of definitions and notations to be extensively used throughout the paper. In Secs. III, IV, and V we describe our all-order calculations of the screened self-energy, the screened vacuum-polarization, and the two-photon exchange corrections, respectively. In Sec. VI we compare the all-order results for the non-mixing states with calculations performed within the $Z\alpha$-expansion approach and identify the remainder of order $m\alpha^7$ and higher. In Sec. VII we describe the comparison of

the two approaches for the mixing $2\,^1P_1$ and $2\,^3P_1$ states and calculate the mixing correction of order $m\alpha^7$ and higher. Finally, Sec. VIII presents our results for the ionization energies and compares theoretical predictions with experimental data. The relativistic units $\hbar = c = 1$ and Heaviside charge units $\alpha = e^2/(4\pi)$ are used in the paper, unless explicitly specified otherwise.

II. DEFINITIONS

Throughout the paper, we will extensively use several basic QED operators: the operator of the electron-electron interaction $I(\omega)$, the one-loop self-energy operator $\Sigma(\varepsilon)$, and the one-loop vacuum-polarization potential $U_{\rm VP}$. The operator of the electron-electron interaction $I(\omega)$ is defined by

$$I(\omega, \boldsymbol{r}_1, \boldsymbol{r}_2) = e^2\, \alpha_1^\mu \alpha_2^\nu\, D_{\mu\nu}(\omega, \boldsymbol{r}_{12})\,, \tag{1}$$

where $\alpha^\mu = (1, \boldsymbol{\alpha})$ are the Dirac matrices, $\boldsymbol{r}_{12} = \boldsymbol{r}_1 - \boldsymbol{r}_2$, and $D_{\mu\nu}(\omega, \boldsymbol{r}_{12})$ is the photon propagator. The one-loop self-energy operator $\Sigma(\varepsilon)$ is defined by its matrix elements with one-electron wave functions $|a\rangle$ and $|b\rangle$ as

$$\langle a|\Sigma(\varepsilon)|b\rangle = \frac{i}{2\pi}\int_{-\infty}^{\infty} d\omega \sum_n \frac{\langle an|I(\omega)|nb\rangle}{\varepsilon - \omega - u\varepsilon_n}\,, \tag{2}$$

where the sum over n is extended over the complete spectrum of the Dirac equation (implying the summation over the discrete states and the integration over the continuum part of the spectrum) and $u = 1 - i\epsilon$ is the infinitesimal addition which ensures the correct position of poles of the electron propagator with respect to the integration contour. The vacuum-polarization potential $U_{\rm VP}$ is given by

$$U_{\rm VP}(\boldsymbol{x}) = \frac{\alpha}{2\pi i}\int_{-\infty}^{\infty} d\omega \int d^3\boldsymbol{y}\, \frac{1}{|\boldsymbol{x} - \boldsymbol{y}|}\, {\rm Tr}\big[G(\omega, \boldsymbol{y}, \boldsymbol{y})\big]\,, \tag{3}$$

where $G(\omega) = (\omega - h_D)^{-1}$ is the Dirac-Coulomb Green function and h_D is the one-electron Dirac-Coulomb Hamiltonian.

In order to simplify the following formulas, we use the following short-hand notations [8] for the summations over the Clebsch-Gordan coefficients in the initial- and the final-state two-electron wave function,

$$F_i|i_1 i_2\rangle \equiv N \sum_{\mu_{i_1}\mu_{i_2}} C^{JM}_{j_{i_1}\mu_{i_1}, j_{i_2}\mu_{i_2}}\, |i_1 i_2\rangle\,, \tag{4}$$

where $|i_1 i_2\rangle$ is the direct product of the one-electron wave functions $|i_1 i_2\rangle = |j_{i_1} l_{i_1} \mu_{i_1}\rangle |j_{i_2} l_{i_2} \mu_{i_2}\rangle$ and N is the normalization factor, $N = 1$ for the non-equivalent electrons ($i_1 \neq i_2$) and $N = 1/\sqrt{2}$ for the case of equivalent electrons ($i_1 = i_2$). We also introduce the permutation operators P and Q that interchange the initial-state and final-state electrons, respectively,

$$\sum_P (-1)^P |P i_1 P i_2\rangle \equiv |i_1 i_2\rangle - |i_2 i_1\rangle\,, \tag{5}$$

$$\sum_Q (-1)^Q |Q k_1 Q k_2\rangle \equiv |k_1 k_2\rangle - |k_2 k_1\rangle\,, \tag{6}$$

where the summation indices P and Q indicates that the summation is carried out over all permutations and $(-1)^P$ and $(-1)^Q$ are the signs of the permutations.

The formulas for the two-electron QED corrections in this paper will be written in the form that is often non-symmetric with respect to the interchange of the initial- and the final-state electron states. It is often the case that the symmetry is preserved and can be proved explicitly. The exception is the case of non-diagonal matrix elements occuring for the mixing $^1P_1$ and $^3P_1$ states; in this case it is assumed that the formulas should be symmetrized with respect $(i_1 i_2) \leftrightarrow (k_1 k_2)$.

We will also use following the shorthand notations: $\Delta_{a,b} = \varepsilon_a - \varepsilon_b$, $I'(\omega) = \partial I(\omega)/(\partial\omega)$, and $\Sigma'(\varepsilon) = \partial\Sigma(\varepsilon)/(\partial\varepsilon)$.

III. SCREENED SELF-ENERGY

The derivation of the general formulas for the screened self-energy correction was presented in Ref. [8]. We here rearrange the formulas in a form suitable for a numerical evaluation. The screened self-energy correction is conveniently represented as a sum of the perturbed-orbital (po), reducible (red), and vertex (ver) contributions,

$$\Delta E_{\rm sescr} = \Delta E_{\rm sescr,po} + \Delta E_{\rm sescr,red} + \Delta E_{\rm sescr,ver}\,. \tag{7}$$

The perturbed-orbital contribution is expressed in terms of diagonal and non-diagonal matrix elements of the one-loop self-energy operator $\Sigma(\varepsilon)$,

$$\Delta E_{\rm sescr,po} = F_i\, F_k \sum_{PQ} (-1)^{P+Q} \Bigg[2 \sum_{n \neq Pi_1} \langle Pi_1|\Sigma(\varepsilon_{Pi_1})|n\rangle\, \frac{\langle nPi_2|I(\Delta_{Qk_2,Pi_2})|Qk_1Qk_2\rangle}{\varepsilon_{Pi_1} - \varepsilon_n} + \langle Pi_1|\Sigma(\varepsilon_{Pi_1})|Pi_1\rangle\, \langle Pi_1 Pi_2|I'(\Delta_{Qk_2,Pi_2})|Qk_1Qk_2\rangle \Bigg]\,, \tag{8}$$

TABLE I. The screened self-energy correction for the $n = 1$ and $n = 2$ states of He-like ions, in units of $\alpha^2(Z\alpha)^3$. "offdiag" labels the off-diagonal $(1s2p_j)_1$ matrix elements of the effective Hamiltonian in the jj-coupling, see text.

Z	$(1s1s)_0$	$(1s2s)_0$	$(1s2s)_1$	$(1s2p_{1/2})_0$	$(1s2p_{1/2})_1$	$(1s2p_{3/2})_1$	$(1s2p_{3/2})_2$	offdiag	
10	−2.410 58 (36)	−0.524 90 (14)	−0.329 31 (11)	−0.101 63 (5)	−0.075 82 (11)	−0.059 00 (11)	−0.145 74 (12)	0.058 372 (12)	
12	−2.213 84 (15)	−0.484 46 (16)	−0.303 28 (5)	−0.091 99 (3)	−0.069 47 (9)	−0.056 00 (9)	−0.135 26 (9)	0.053 223 (7)	
14	−2.054 26 (9)	−0.451 78 (10)	−0.282 14 (3)	−0.084 39 (4)	−0.064 45 (9)	−0.053 61 (9)	−0.126 75 (7)	0.049 049 (6)	
16	−1.921 71 (9)	−0.424 79 (9)	−0.264 54 (3)	−0.078 30 (4)	−0.060 43 (8)	−0.051 69 (8)	−0.119 69 (7)	0.045 582 (3)	
18	−1.809 65 (8)	−0.402 13 (7)	−0.249 63 (4)	−0.073 36 (4)	−0.057 15 (6)	−0.050 12 (6)	−0.113 73 (7)	0.042 648 (2)	
20	−1.713 71 (6)	−0.382 86 (3)	−0.236 82 (2)	−0.069 32 (2)	−0.054 46 (3)	−0.048 82 (4)	−0.108 63 (4)	0.040 129 (2)	
	−1.713 72 (8)	−0.382 86 (3)	−0.236 82 (3)	−0.069 32 (3)	−0.054 46 (3)	−0.048 83 (3)	−0.108 63 (3)	0.040 129 (1)	Coulomb
	−1.713 7 (3)	−0.382 8 (3)	−0.236 8 (3)	−0.069 3 (1)	−0.054 4 (1)	−0.048 8 (2)	−0.108 6 (2)	0.040 13 (3)	Ref. [8]
	−1.713 4 (3)								Ref. [7]
24	−1.558 27 (6)	−0.352 04 (4)	−0.215 97 (2)	−0.063 33 (2)	−0.050 46 (3)	−0.046 88 (3)	−0.100 35 (5)	0.036 020 (2)	
28	−1.438 56 (7)	−0.328 85 (3)	−0.199 79 (1)	−0.059 41 (1)	−0.047 83 (2)	−0.045 58 (3)	−0.093 96 (4)	0.032 811 (3)	
30	−1.388 86 (4)	−0.319 43 (1)	−0.193 02 (1)	−0.058 06 (1)	−0.046 93 (2)	−0.045 12 (3)	−0.091 31 (4)	0.031 457 (1)	
	−1.388 8 (2)	−0.319 4 (2)	−0.193 0 (2)	−0.058 1 (1)	−0.047 0 (1)	−0.045 2 (2)	−0.091 3 (2)	0.031 46 (2)	Ref. [8]
	−1.388 9 (3)								Ref. [7]
32	−1.344 72 (3)	−0.311 22 (2)	−0.186 99 (1)	−0.057 05 (1)	−0.046 25 (1)	−0.044 77 (2)	−0.088 94 (4)	0.030 239 (1)	
36	−1.270 43 (3)	−0.297 88 (1)	−0.176 77 (1)	−0.055 95 (1)	−0.045 49 (1)	−0.044 33 (2)	−0.084 94 (4)	0.028 138 (1)	
40	−1.211 48 (1)	−0.287 96 (1)	−0.168 57 (1)	−0.055 89 (1)	−0.045 42 (1)	−0.044 19 (2)	−0.081 72 (2)	0.026 393 (1)	

where the summation over n is performed over the complete Dirac spectrum. The reducible part of the screened self-energy correction contains the derivative of the self-energy operator and is given by

$$\Delta E_{\rm sescr,red} = F_i\, F_k \sum_{PQ} (-1)^{P+Q} \langle Pi_1|\Sigma'(\varepsilon_{Pi_1})|Pi_1\rangle\, \langle Pi_1 Pi_2|I(\Delta_{Qk_2,Pi_2})|Qk_1 Qk_2\rangle\,. \tag{9}$$

The vertex part of the screened self-energy correction is

$$\Delta E_{\rm sescr,ver} = F_i\, F_k \sum_{PQ} (-1)^{P+Q} \frac{i}{2\pi} \int_{-\infty}^{\infty} d\omega \sum_{n_1 n_2} \frac{\langle Pi_1 n_2|I(\omega)|n_1 Qk_1\rangle\, \langle n_1 Pi_2|I(\Delta_{Qk_2,Pi_2})|n_2 Qk_2\rangle}{(\varepsilon_{Pi_1} - \omega - u\,\varepsilon_{n_1})(\varepsilon_{Qk_1} - \omega - u\,\varepsilon_{n_2})}\,. \tag{10}$$

The numerical evaluation of the screened self-energy corrections is based on the use of the analytical representation of the Dirac-Coulomb Green function in terms of the Whittaker functions, see Ref. [20] for details. The perturbed-orbital contribution $\Delta E_{\rm po}$ is expressed in terms of diagonal and non-diagonal matrix elements of the one-loop self-energy operator $\Sigma(\varepsilon)$, which are computed by numerical methods described in detail in Refs. [21, 22]. The general scheme of evaluation of the reducible and vertex corrections was developed in Ref. [23]. The contributions of the free electron propagators are separated out and calculated in the momentum space, after a covariant regularization of ultraviolet divergences and an explicit cancellation of divergent terms. The remaining (many-potential) contributions contain infrared-divergent terms, arising when the energy differences in the energy denominators vanish (e.g., in Eq. (10) with $n_1 = Pi_1$ and $n_2 = Qk_1$). The divergent terms in the vertex and reducible contributions are separated out and regularized by introducing a finite photon mass. The divergencies cancel out in the sum of the vertex and the reducible contributions (see Appendix B of Ref. [20] for details), leaving a finite remainder to be calculated numerically.

The many-potential reducible contribution was computed as a derivative of the one-loop self-energy operator by the method developed in Ref. [22]. The many-potential vertex contribution contains two bound electron propagators and represents the main computational difficulty. In the present work, we evaluate it with the technique described in detail in Ref. [20], which was recently employed for the evaluation of the self-energy screening corrections to the g factor [24]. The expansion over the partial waves in the vertex term is the main source of the numerical uncertainty. It was extended up to $|\kappa_{\rm max}| = 50$, with the remainder of the tail estimated by a polynomial fitting of the expansion terms in $1/|\kappa|$.

Numerical results of our computations of the screened self-energy correction are presented in Table I in terms of the scaled function $G_{\rm sescr}(Z\alpha)$, with the leading α and $Z\alpha$ dependence pulled out,

$$\Delta E_{\rm sescr} = m\alpha^2(Z\alpha)^3\, G_{\rm sescr}(Z\alpha)\,. \tag{11}$$

Results in Table I are obtained for the point nuclear charge model and, unless explicitly specified, in the Feynman gauge. For $Z = 20$, results are presented also for the Coulomb gauge for the photon connecting the two electrons. In the case of the mixing $(1s2p_j)_1$ configurations, contributions to the matrix elements of the effective Hamiltonian in the jj-coupling are presented, see Sec. VII. The off-diagonal $(1s2p_j)_1$ matrix elements are listed under the label "offdiag".

The comparison presented in Table I shows that our present results are in good agreement with those from previous computations [7, 8] but are more accurate. It is also demonstrated

that our numerical results are gauge invariant well within the estimated numerical uncertainty.

IV. SCREENED VACUUM-POLARIZATION

The derivation of the general formulas for the screened vacuum-polarization correction was presented in Ref. [8]. We now summarize the final formulas needed for the actual calculation. The screened vacuum-polarization correction is conveniently represented as a sum of the perturbed-orbital (po), and the photon-propagator (ph) contributions,

$$\Delta E_{\rm vpscr} = \Delta E_{\rm vpscr,po} + \Delta E_{\rm vpscr,ph}\,. \tag{12}$$

The perturbed-orbital contribution is analogous to that for the screened self-energy and is expressed in terms of matrix elements of the one-loop vacuum-polarization potential,

$$\Delta E_{\rm vpscr,po} = F_i\,F_k \sum_{PQ} (-1)^{P+Q} \Bigg[2 \sum_{n\neq Pi_1} \langle Pi_1|U_{\rm VP}|n\rangle\, \frac{\langle nPi_2|I(\Delta_{Qk_2,Pi_2})|Qk_1Qk_2\rangle}{\varepsilon_{Pi_1}-\varepsilon_n} + \langle Pi_1|U_{\rm VP}|Pi_1\rangle\, \langle Pi_1Pi_2|I'(\Delta_{Qk_2,Pi_2})|Qk_1Qk_2\rangle \Bigg]\,. \tag{13}$$

The remaining part of the screened vacuum-polarization is given by the correction to the photon propagator,

$$\Delta E_{\rm vpscr,ph} = F_i\,F_k \sum_{PQ} (-1)^{P+Q} \langle Pi_1Pi_2|U_{\rm ph}(\Delta_{Qk_2,Pi_2})|Qk_1Qk_2\rangle\,, \tag{14}$$

where $U_{\rm ph}$ is the radiatively-corrected photon propagator,

$$U_{\rm ph}(\delta,\boldsymbol{x},\boldsymbol{y}) = \frac{\alpha^2}{2\pi i}\int_{-\infty}^{\infty} d\omega \int d^3\boldsymbol{z}_1 d^3\boldsymbol{z}_2\, \alpha_\mu\, D^{\mu\nu}(\delta,\boldsymbol{x},\boldsymbol{z}_1)\,{\rm Tr}\Big[\alpha_\nu\, G(\omega-\delta/2,\boldsymbol{z}_1,\boldsymbol{z}_2)\,\alpha_\rho\, G(\omega+\delta/2,\boldsymbol{z}_2,\boldsymbol{z}_1)\Big] D^{\rho\sigma}(\delta,\boldsymbol{z}_2,\boldsymbol{y})\,\alpha_\sigma\,. \tag{15}$$

The screened vacuum-polarization correction was first calculated for the ground state of He-like ions in Refs. [5, 6] and for the $n=2$ excited states in Ref. [8]. The numerical calculation of the present work follows the general scheme developed in these studies. The Wichmann-Kroll part of the vacuum-polarization potential $U_{\rm VP}$ was computed for the point nuclear charge with help of approximate formulas obtained in Refs. [25–27]. The summation over the Dirac spectrum in Eq. (13) causes no problem and can be computed in different ways. In the present work we chose to use the B-splines basis set method [28], which is technically the simplest choice in this case.

The vacuum-polarization correction to the photon propagator is standardly separated into the Uehling and the Wichmann-Kroll parts [6]. The calculation of the Uehling part is relatively straightforward and was performed by formulas from Ref. [6]. The Wichmann-Kroll part of the radiatively-corrected photon propagator is more difficult to compute but its contribution is very small for the range of the nuclear charges considered in the present work. We therefore exclude this correction from our calculation, estimating its upper bound to make sure that it does not contribute on the level of our present interest. For the largest Z considered in this work, $Z=40$, we estimate the contribution to the function $G_{\rm vpscr}$ to be less than 1×10^{-4} for the $(1s)^2$ state and less than 1×10^{-5} for the $n=2$ states [29]. As Z decreases, the contribution diminishes quickly and can be completely ignored in the context of the present investigation.

Our numerical results for the screened vacuum-polarization correction are presented in Table II in terms of the scaled function $G_{\rm vpscr}(Z\alpha)$ defined as

$$\Delta E_{\rm vpscr} = m\alpha^2 (Z\alpha)^3\, G_{\rm vpscr}(Z\alpha)\,. \tag{16}$$

The comparison presented in the table shows that our results are in agreement with previous calculations [6, 8].

V. TWO-PHOTON EXCHANGE

The two-photon exchange correction was first calculated for the ground state of He-like ions in Ref. [30]. Calculations for the $n=2$ excited states were performed independently by several groups over the course of several decades [8, 9, 31–34].

We here follow the approach of Ref. [8] and express the two-photon exchange correction as a sum of the irreducible (ir) and the reducible (red) contributions,

$$\Delta E_{\rm 2ph} = \Delta E_{\rm 2ph,ir} + \Delta E_{\rm 2ph,red}\,. \tag{17}$$

TABLE II. The screened vacuum-polarization correction for the $n = 1$ and $n = 2$ states of He-like ions, in units $\alpha^2(Z\alpha)^3$.

Z	$(1s1s)_0$	$(1s2s)_0$	$(1s2s)_1$	$(1s2p_{1/2})_0$	$(1s2p_{1/2})_1$	$(1s2p_{3/2})_1$	$(1s2p_{3/2})_2$	offdiag	
10	0.117 77	0.024 78	0.016 87	0.006 95	0.004 27	0.001 60	0.006 82	−0.003 714	
12	0.117 30	0.024 73	0.016 74	0.006 94	0.004 27	0.001 59	0.006 76	−0.003 679	
14	0.117 04	0.024 73	0.016 65	0.006 95	0.004 27	0.001 59	0.006 70	−0.003 650	
16	0.116 99	0.024 78	0.016 58	0.006 97	0.004 29	0.001 59	0.006 65	−0.003 626	
18	0.117 13	0.024 88	0.016 53	0.007 02	0.004 31	0.001 59	0.006 61	−0.003 607	
20	0.117 47	0.025 03	0.016 51	0.007 08	0.004 35	0.001 60	0.006 58	−0.003 592	
	0.117	0.025	0.017	0.007	0.005	0.001	0.007	−0.004	Ref. [8]
24	0.118 7	0.025 48	0.016 53	0.007 26	0.004 45	0.001 61	0.006 53	−0.003 575	
28	0.120 7	0.026 13	0.016 64	0.007 52	0.004 60	0.001 64	0.006 50	−0.003 574	
30	0.122 0	0.026 54	0.016 73	0.007 67	0.004 70	0.001 65	0.006 49	−0.003 579	
	0.122	0.026 6	0.016 8	0.007 7	0.004 6	0.001 8	0.006 7	−0.003 5	Ref. [8]
32	0.123 4	0.026 99	0.016 84	0.007 85	0.004 80	0.001 66	0.006 49	−0.003 588	
36	0.126 9	0.028 07	0.017 13	0.008 28	0.005 06	0.001 70	0.006 50	−0.003 615	
40	0.131 2	0.029 38	0.017 52	0.008 81	0.005 37	0.001 74	0.006 54	−0.003 657	

The irreducible part is given by

$$\Delta E_{2\mathrm{ph,ir}} = F_i\, F_k \sum_P (-1)^P \frac{i}{2\pi} \int_{-\infty}^{\infty} d\omega \left\{ \sum_{n_1 n_2}^{E_n \neq E^{(0)}} \frac{\langle Pi_1 Pi_2|I(\omega)|n_1 n_2\rangle \, \langle n_1 n_2|I(\omega-\Delta_{k_1,Pi_1})|k_1 k_2\rangle}{(\varepsilon_{Pi_1}+\omega-u\varepsilon_{n_1})(\varepsilon_{Pi_2}-\omega-u\varepsilon_{n_2})} + \sum_{n_1 n_2} \frac{\langle Pi_1 n_2|I(\omega)|n_1 k_2\rangle \, \langle n_1 Pi_2|I(\omega-\Delta_{k_1,Pi_1})|k_1 n_2\rangle}{(\varepsilon_{Pi_1}+\omega-u\varepsilon_{n_1})(\varepsilon_{k_2}+\omega-u\varepsilon_{n_2})} \right\}, \tag{18}$$

where $E_n = \varepsilon_{n_1} + \varepsilon_{n_2}$ and $E^{(0)}$ is the energy of the reference state. The condition $E_n \neq E^{(0)}$ for excluding intermediate states from the summation over n_1 and n_2 in the above formula should be understood differently for the case of non-mixing and the case of mixing states. In the former case (in this work, for all states except $2\,^1P_1$ and $2\,^3P_1$), the reference state correspond to an isolated level, with $E^{(0)} = \varepsilon_{i_1} + \varepsilon_{i_2} = \varepsilon_{k_1} + \varepsilon_{k_2}$. The terms to be excluded from the summation are thus $(n_1, n_2) = (i_1, i_2)$ and (i_2, i_1). In the latter case, the reference state belongs to a sub-space of quasidegenerate levels (in this work, the $2\,^1P_1$ and $2\,^3P_1$ states) and one should exclude all of them from the summation, $(n_1, n_2) = (1s, 2p_{1/2})$, $(1s, 2p_{3/2})$, $(2p_{1/2}, 1s)$, $(2p_{3/2}, 1s)$.

The reducible part accounts for the terms excluded from the summation over n_1 and n_2 in the irreducible part. It is given by

$$\Delta E_{2\mathrm{ph,red}} = F_i\, F_k \sum_P (-1)^P \frac{i}{4\pi} \int_{-\infty}^{\infty} d\omega \sum_{n_1 n_2}^{E_n = E^{(0)}} \langle Pi_1 Pi_2|I(\omega)|n_1 n_2\rangle \, \langle n_1 n_2|I(\omega-\Delta_{k_1,Pi_1})|k_1 k_2\rangle \times \left[\frac{1}{(\varepsilon_{Pi_1}+\omega-\varepsilon_{n_1}+i0)(\varepsilon_{Pi_2}-\omega-\varepsilon_{n_2}-i0)} + \frac{1}{(\varepsilon_{Pi_1}+\omega-\varepsilon_{n_1}-i0)(\varepsilon_{Pi_2}-\omega-\varepsilon_{n_2}+i0)} \right]. \tag{19}$$

It might be noted that the terms in the reducible part have the same form as the terms excluded from the summation in the irreducible part but differ from them by signs of the infinitesimal imaginary additions in the pole positions. Note also that formulas for the quasidegenerate states have some arbitrariness in them, which corresponds to a possibility to re-assign small contributions to higher orders of perturbation theory [35]. In particular, authors of Ref. [9] used a different choice of the reference-state energy. This arbitrariness leads to very small numerical changes in the results.

The numerical evaluation of the two-photon exchange corrections is rather involved, but relatively well established at present. Unlike the self-energy correction computed with help of the analytical representation of the Dirac-Coulomb Green function, all previous computations of the two-photon exchange [8, 9, 31–34] were performed using the spectral representation of the Green function, with help of the B-spline finite basis set method [28]. The reason behind this is purely technical. First, the radial integrations are more efficiently computed in the spectral representation. Second, the computation of the ω integration along the contour extending near poles of the electron propagator is easier implemented for the spectral representation of the Green function.

In the present work we follow the previous studies and use the B-spline finite basis set method [28] for the evaluation of the two-photon exchange correction. We note that we do not

TABLE III. The two-photon exchange correction for the ground and $n = 2$ states of He-like ions, in eV.

Z	$(1s1s)_0$	$(1s2s)_0$	$(1s2s)_1$	$(1s2p_{1/2})_0$	$(1s2p_{1/2})_1$	$(1s2p_{3/2})_1$	$(1s2p_{3/2})_2$	offdiag	
10	−4.380 311 (7)	−3.156 509 (4)	−1.296 332 (2)	−2.030 796 (3)	−2.769 646 (1)	−3.526 412 (2)	−1.993 318 (2)	−1.073 247 (7)	
12	−4.419 431 (11)	−3.174 334 (5)	−1.299 108 (2)	−2.050 558 (5)	−2.778 965 (2)	−3.533 294 (2)	−1.996 368 (3)	−1.071 185 (4)	
14	−4.465 463 (15)	−3.195 431 (7)	−1.302 403 (3)	−2.074 088 (6)	−2.790 022 (2)	−3.541 435 (3)	−1.999 973 (3)	−1.068 737 (5)	
16	−4.518 375 (18)	−3.219 828 (8)	−1.306 222 (3)	−2.101 472 (7)	−2.802 838 (3)	−3.550 839 (3)	−2.004 131 (4)	−1.065 905 (9)	
18	−4.578 150 (23)	−3.247 563 (10)	−1.310 572 (4)	−2.132 807 (8)	−2.817 439 (3)	−3.561 515 (4)	−2.008 838 (5)	−1.062 686 (6)	
20	−4.644 780 (27)	−3.278 681 (12)	−1.315 460 (5)	−2.168 207 (9)	−2.833 853 (3)	−3.573 469 (4)	−2.014 093 (5)	−1.059 080 (7)	
	−4.644 769 (18)	−3.278 679 (12)	−1.315 460 (5)	−2.168 207 (9)	−2.833 853 (5)	−3.573 468 (9)	−2.014 093 (5)	−1.059 079 (13)	Coulomb
	−4.644 76 (19)	−3.278 67 (3)	−1.315 457 (4)	−2.168 20 (2)	−2.833 85 (2)	−3.573 46 (5)	−2.014 088 (10)	−1.059 07 (5)	Ref. [9]
	−4.643 5	−3.278 4	−1.315 4	−2.168 2	−2.833 7	−3.573 3	−2.014 1	−1.058 9	Ref. [8]
24	−4.798 626 (37)	−3.351 293 (16)	−1.326 883 (6)	−2.251 724 (10)	−2.872 262 (4)	−3.601 255 (5)	−2.026 227 (6)	−1.050 710 (8)	
28	−4.980 080 (50)	−3.438 206 (21)	−1.340 564 (8)	−2.353 222 (11)	−2.918 384 (4)	−3.634 290 (6)	−2.040 495 (6)	−1.040 797 (10)	
30	−5.081 262 (57)	−3.487 234 (23)	−1.348 279 (9)	−2.411 161 (12)	−2.944 458 (4)	−3.652 811 (7)	−2.048 415 (6)	−1.035 263 (10)	
	−5.081 22 (17)	−3.487 20 (5)	−1.348 270 (3)	−2.411 14 (2)	−2.944 45 (5)	−3.652 80 (10)	−2.048 399 (10)	−1.035 21 (3)	Ref. [9]
	−5.079 5	−3.486 8	−1.348 3	−2.411 1	−2.944 3	−3.652 5	−2.048 4	−1.035 0	Ref. [8]
	−5.081 18	−3.487 164	−1.348 268						Refs. [33, 36]
32	−5.189 494 (65)	−3.540 110 (26)	−1.356 593 (10)	−2.474 167 (13)	−2.972 615 (4)	−3.672 691 (7)	−2.056 851 (6)	−1.029 347 (11)	
36	−5.427 426 (82)	−3.657 867 (32)	−1.375 072 (12)	−2.616 323 (14)	−3.035 439 (5)	−3.716 601 (9)	−2.075 246 (7)	−1.016 373 (13)	
40	−5.694 644 (99)	−3.792 523 (38)	−1.396 126 (14)	−2.781 799 (16)	−3.107 442 (5)	−3.766 186 (10)	−2.095 623 (7)	−1.001 890 (15)	

use the the dual-kinetical-balance (DKB) basis set [37] since we perform calculations for the point nuclear charge, while the DKB method is formulated for an extended nuclear-charge model only. The numerical procedure used in this work is very similar to the one developed for the two-photon exchange correction to the bound-electron g factor and described in detail in Ref. [38]. The computation was performed in two gauges, the Feynman and the Coulomb one. The results obtained in the two gauges agree well within the estimated numerical uncertainty.

The computation of the two-photon exchange correction needs to be performed to a very high numerical accuracy, because of the presence of the nonrelativistic ($\sim (Z\alpha)^0$) and relativistic ($\sim (Z\alpha)^2$) contributions. The QED part of the two-photon exchange enters in the order $(Z\alpha)^3$ only; its identification thus entails severe numerical cancellations in the low-Z region. By contrast, the screened self-energy and vacuum-polarization corrections scale as $(Z\alpha)^3$, so their numerical uncertainty is less crucial for the determination of the total two-electron QED correction.

The dominant sources of numerical uncertainty for the two-photon exchange correction are the convergence with respect to the number of basis functions N and the truncation of the partial-wave expansion. Our calculations were performed typically for several sets of B-splines with N up to $N = 125$ and then extrapolated to $N \to \infty$. The infinite partial-wave summation over the relativistic angular momentum quantum number κ was extended up to $|\kappa_{\max}| = 25$, with the remaining tail estimated by the polynomial fitting of the expansion terms in $1/|\kappa|$.

Numerical results of our calculation are summarized in Table III. They are obtained for the point nuclear charge distribution and, unless explicitly specified, the Feynman gauge. For $Z = 20$, we present in addition results obtained in the Coulomb gauge. The comparison presented in the table shows that our values are in good agreement with results obtained previously but are more accurate.

TABLE IV. Coefficients of the $Z\alpha$ expansion of the two-photon exchange correction.

	a_{20}	a_{40}
$1\,^1S_0$	−0.157 666 43	−0.636 506 9
$2\,^1S_0$	−0.114 510 14	−0.281 858 6
$2\,^3S_1$	−0.047 409 30	−0.042 775 5
$2\,^1P_1$	−0.157 028 66	−0.090 632 2
$2\,^3P_0$	−0.072 998 98	−0.303 523 4
$2\,^3P_1$	−0.072 998 98	−0.162 129 4
$2\,^3P_2$	−0.072 998 98	−0.047 315 7
$(2\,^1P_1, 2\,^3P_1)$	0	−0.004 718 5

VI. HIGHER-ORDER QED: NON-MIXING STATES

We now turn to comparing our present calculations performed to all orders in $Z\alpha$ with results obtained in the framework of the $Z\alpha$ expansion. After the agreement of the two approaches is demonstrated, we will proceed to indentifying the higher-order QED remainder that can be added to the results of the NRQED calculations of Ref. [14]. We start with the non-mixing states, i.e., the ground and all $n = 2$ states except $2\,^1P_1$ and $2\,^3P_1$.

A. Comparison with $Z\alpha$ expansion

In order to identify the QED part of our all-order results, we need first to remove the nonrelativistic and relativistic contributions from the two-photon exchange correction. The QED part of the two-photon exchange is given by the function $G_{2\mathrm{ph}}$ defined as

$$\Delta E_{2\mathrm{ph}} = m\alpha^2 \left[a_{20} + (Z\alpha)^2\, a_{40} + (Z\alpha)^3\, G_{2\mathrm{ph}}(Z\alpha)\right] . \tag{20}$$

Here the coefficient a_{20} arises from the Z^{-2} term of the $1/Z$ expansion of the nonrelativistic energy, whereas a_{40} comes

TABLE V. Coefficients of the $Z\alpha$ expansion of the one-loop two-electron QED correction.

	a_{51}	a_{50}	a_{61}	a_{60}	a_{72}	a_{71}
$1\,^1S$	−0.659 550 48	1.658 816 0	$1/16$	−4.3711	0.425 033	
$2\,^1S$	−0.137 744 61	0.325 517 0	$1/81$	−1.1041	0.089 554	
$2\,^3S$	−0.089 756 44	0.191 147 5	0	−0.6514	0.067 317	−0.4829
$2\,^1P_1$	0.003 158 46	−0.017 559 8	$1/243$	0.0062	−0.006 954	
$2\,^3P_0$	−0.036 478 76	0.106 210 2	0	−0.6796	0.027 359	−0.3681
$2\,^3P_1$	−0.036 478 76	0.081 192 9	0	−0.3088	0.027 359	−0.3171
$2\,^3P_2$	−0.036 478 76	0.059 452 5	0	−0.2117	0.027 359	−0.2556
$(2\,^1P_1, 2\,^3P_1)$	0	0.011 962 3	0			

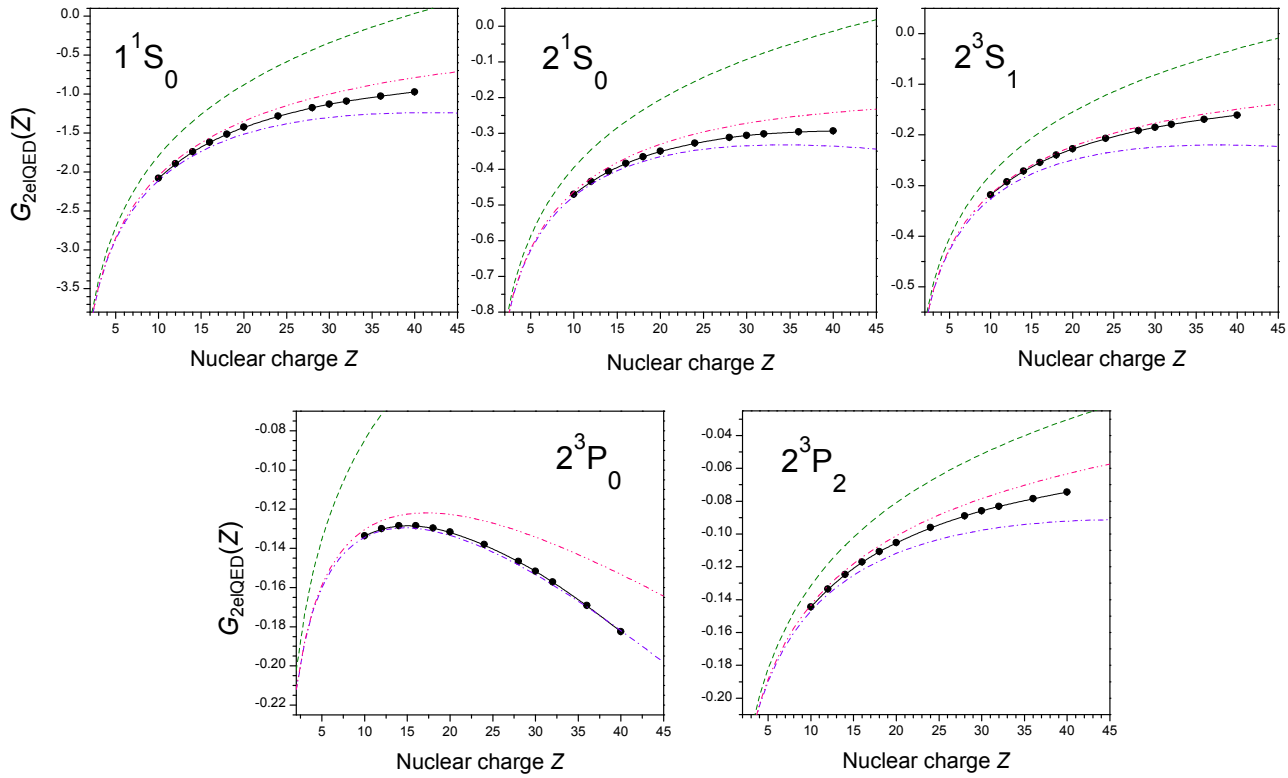

FIG. 1. The two-electron QED correction for non-mixing states of He-like ions, as a function of the nuclear charge number Z, in terms of the function $G_{\rm 2elQED}$ defined by Eq. (21). The dots and solid line (black) present results of all-order numerical calculation. The dashed line (green) shows the contribution of the leading $Z\alpha$-expansion term of order $\alpha^2(Z\alpha)^3$; the dashed-dotted line (violet) is the contribution of two first $Z\alpha$-expansion terms of order $\alpha^2(Z\alpha)^3$ and $\alpha^2(Z\alpha)^4$; the double-dotted dashed line (pink) shows the contribution of two first $Z\alpha$-expansion terms plus the hydrogenic estimate of the higher-order terms.

from the Z^{-2} term of the $1/Z$ expansion of the Breit correction $\sim m\alpha^4$. The function $G_{\rm 2ph}(Z\alpha)$ contains terms of order $m\alpha^5$ and higher. Numerical results for the coefficients a_{20} and a_{40} were obtained in Ref. [14] and are summarized in Table IV.

The total two-electron QED correction is defined as the sum of the self-energy, vacuum-polarization, and two-photon-exchange parts,

$$\Delta E_{\rm 2elQED} \equiv m\alpha^2\,(Z\alpha)^3\,G_{\rm 2elQED}(Z\alpha) = m\alpha^2\,(Z\alpha)^3\left[G_{\rm sescr} + G_{\rm vpscr} + G_{\rm 2ph}\right]. \quad (21)$$

It should be noted that the above definition of the two-electron QED contribution includes only one-loop effects. It does not include the two-loop correction, for which no all-order calculations have been performed so far. The $Z\alpha$-expansion of the function $G_{\rm 2elQED}$ reads

$$G_{\rm 2elQED}(Z\alpha) = L\,a_{51} + a_{50} + \alpha L\,a_{61} + (Z\alpha)\,a_{60} + (Z\alpha)^2\,G^{(7+)}_{\rm 2elQED}\,, \quad (22)$$

where $L \equiv \ln(Z\alpha)^{-2}$ and $G^{(7+)}_{\rm 2elQED}$ is the higher-order remainder,

$$G^{(7+)}_{\rm 2elQED}(Z\alpha) = L^2\,a_{72} + L\,a_{71} + a_{70} + (Z\alpha)L\,a_{81} + \ldots\,. \quad (23)$$

TABLE VI. The higher-order QED and finite nuclear size (FNS) contributions for the ground and the non-mixing $n = 2$ states. Units are $m\alpha^2(Z\alpha)^5$.

Z	$1/Z^0$	$1/Z^1$	$1/Z^{2+}$	FNS	Total
1^1S					
6	−67.917	7.105	−0.670	9.354	−52.13 (60)
8	−78.259	6.447	−0.433	9.022	−63.22 (36)
10	−87.192	5.964	−0.308	9.411	−72.12 (27)
14	−102.405	5.304	−0.184	7.836	−89.45 (17)
18	−115.469	4.911	−0.124	7.856	−102.83 (12)
20	−121.511	4.786	−0.106	7.533	−109.30 (11)
24	−133.013	4.641	−0.079	7.405	−121.046 (91)
28	−144.127	4.609	−0.062	7.354	−132.226 (83)
30	−149.658	4.629	−0.056	7.731	−137.354 (80)
2^1S					
6	−7.967	1.320	−0.353	0.993	−6.01 (33)
8	−9.182	1.168	−0.230	1.002	−7.24 (21)
10	−10.246	1.079	−0.164	1.075	−8.26 (15)
14	−12.119	0.989	−0.098	0.925	−10.303 (87)
18	−13.831	0.962	−0.066	0.948	−11.987 (58)
20	−14.670	0.966	−0.056	0.917	−12.843 (49)
24	−16.380	1.001	−0.042	0.917	−14.504 (38)
28	−18.197	1.070	−0.033	0.925	−16.236 (30)
30	−19.170	1.115	−0.030	0.980	−17.104 (28)
2^3S					
6	−7.967	2.041	−0.122	1.090	−4.958 (41)
8	−9.182	1.757	−0.078	1.075	−6.428 (34)
10	−10.246	1.565	−0.055	1.137	−7.601 (31)
14	−12.119	1.321	−0.033	0.963	−9.868 (18)
18	−13.831	1.179	−0.022	0.978	−11.696 (14)
20	−14.670	1.131	−0.019	0.943	−12.615 (13)
24	−16.380	1.064	−0.014	0.938	−14.391 (12)
28	−18.197	1.028	−0.011	0.943	−16.237 (12)
30	−19.170	1.019	−0.010	0.998	−17.163 (11)
2^3P_0					
6	0.615	0.280	−0.234	−0.128	0.53 (26)
8	0.707	0.249	−0.150	−0.094	0.71 (18)
10	0.763	0.243	−0.106	−0.078	0.82 (13)
14	0.764	0.276	−0.063	−0.045	0.931 (77)
18	0.602	0.351	−0.043	−0.034	0.876 (53)
20	0.450	0.401	−0.036	−0.028	0.787 (46)
24	−0.016	0.525	−0.027	−0.020	0.462 (35)
28	−0.732	0.679	−0.021	−0.014	−0.088 (29)
30	−1.196	0.768	−0.019	−0.012	−0.460 (26)
2^3P_2					
6	0.381	0.661	−0.234	−0.129	0.68 (11)
8	0.456	0.559	−0.151	−0.095	0.769 (79)
10	0.518	0.489	−0.107	−0.080	0.821 (60)
14	0.625	0.400	−0.063	−0.048	0.914 (36)
18	0.711	0.348	−0.043	−0.037	0.979 (25)
20	0.748	0.329	−0.036	−0.032	1.009 (21)
24	0.812	0.301	−0.027	−0.026	1.060 (16)
28	0.865	0.282	−0.021	−0.022	1.103 (13)
30	0.888	0.275	−0.019	−0.022	1.121 (12)

The coefficients a_{51}, a_{50}, and a_{61} were obtained in Ref. [14] by fitting the $1/Z$ expansion of the NRQED results. The coefficient a_{60} was also obtained in Ref. [14], but for our present purposes it needed to be reevaluated to exclude the two-loop contribution. The coefficient a_{72} is proportional to the Dirac δ function and is immediately obtained from the hydrogen theory. Specifically, a_{72} is induced by the self-energy coefficient $A_{62}(ns) = -1$, see Eq. (8) of Ref. [39],

$$a_{72} = A_{62}\,\frac{c_1}{\pi} = -\frac{c_1}{\pi}\,, \tag{24}$$

where c_1 is the $1/Z^1$ coefficient of the $1/Z$ expansion of the matrix element of the Dirac δ function,

$$\left\langle \frac{\pi}{Z^3}\left[\delta^3(r_1)+\delta^3(r_2)\right]\right\rangle = c_0 + \frac{c_1}{Z} + \frac{c_2}{Z^2} + \dots\,. \tag{25}$$

The coefficients c_i for the $n = 1$ and $n = 2$ states of He-like ions are given in Table I of Ref. [13]. The coefficient a_{71} for the triplet states is evaluated in the present work, on the basis of formulas derived in Ref. [16]. For the singlet states, a_{71} is unknown. The nonlogarithmic $m\alpha^7$ correction was evaluated in Ref. [16] for helium; no results for its $1/Z$ expansion coefficients were reported yet. The logarithmic coefficient in the next order, a_{81}, is also proportional to the Dirac δ function and thus can be obtained from the hydrogen theory. Specifically, $a_{81} = (427/192 - \ln 2)\,c_1$ [40, 41]. The summary of all known $Z\alpha$-expansion coefficients is given in Table V.

In Fig. 1 we present a comparison of our all-order calculations of the two-electron QED contribution with predictions based on the $Z\alpha$ expansion. We conclude that the all-order results in the low-Z region converge to the predictions of the $Z\alpha$ expansion and that the difference is consistent with the expected magnitude of higher-order effects.

After checking the consistency of our all-order calculations with the known terms of the $Z\alpha$ expansion, we are now in a position to obtain numerical results for the higher-order remainder function $G^{(7+)}_{\rm 2elQED}$ defined by Eq. (22), by subtracting contributions of lower orders in $Z\alpha$ from the all-order results. Since our numerical calculations are performed for $Z \geq 10$, we have to use an extrapolation in order to get results for smaller values of Z. The extrapolation is complicated by the presence of logarithms in the expansion of the function. For the triplet states, we make use of the NRQED results for the logarithmic coefficients a_{72}, a_{71}, and a_{81} in order to improve the accuracy of the extrapolation. Specifically, we subtract all known logarithmic terms, apply a polynomial extrapolation, and then re-add the logarithmic terms back. For the singlet states, the logarithmic coefficient a_{71} is not known, so we had to include the single logarithmic term into the fitting function. For this reason, the accuracy of the fit was lower for the singlet than for the triplet states.

B. Higher-order QED contribution

The calculation of all QED effects up to order $m\alpha^6$ to energies of the $n = 1$ and $n = 2$ states of light He-like ions was

performed in Ref. [14]. These results needed to be complemented with a separate treatment of the higher-order effects of order $m\alpha^7$ and higher.

The higher-order QED contribution to the ionization energy of a $1snl_j$ state was evaluated in Ref. [14] as a sum of three parts,

$$E^{(7+)} = E_D^{(7+)} + E_{\rm 1ph}^{(7+)} + E_{\rm rad}^{(7+)}\,, \tag{26}$$

where the first term is the higher-order part of the Dirac energy of the nl_j one-electron state, the second term is the higher-order part of the one-photon exchange correction, and the third term is the higher-order part of the radiative QED correction. The first two terms are readily evaluated numerically, whereas the radiative QED contribution was evaluated in Ref. [14] by rescaling the hydrogenic result with the expectation value of the Dirac δ function. Specifically, the following expression was used:

$$E_{\rm rad}^{(7+)} = \Big[E_{\rm rad,H}^{(7+)}(1s) + E_{\rm rad,H}^{(7+)}(nl_j)\Big] \times \frac{\left\langle \frac{\pi}{Z^3}\big[\delta^3(r_1)+\delta^3(r_2)\big]\right\rangle}{1+\frac{\delta_{l,0}}{n^3}} - E_{\rm rad,H}^{(7+)}(1s)\,, \tag{27}$$

where $E_{\rm rad,H}^{(7+)}(nl_j)$ is the hydrogenic radiative correction of order of $m\alpha^7$ and higher. The approximation of Eq. (27) is sometimes referred to as the hydrogenic approximation.

Formula (27) is exact to the leading (zeroth) order in $1/Z$ but only approximate to higher orders in $1/Z$. In the present work, we calculated the two-electron QED correction to all orders in $Z\alpha$. With this calculation, we can improve on Eq. (27) and make it exact to the first order in $1/Z$ for the dominant one-loop effects. We obtain the additional contribution to be added to Eq. (27) as

$$E_{\rm add}^{(7+)} = G_{\rm 2elQED}^{(7+)} - \Big[E_{\rm 1loop,H}^{(7+)}(1s) + E_{\rm 1loop,H}^{(7+)}(nl_j)\Big]\,\frac{c_1}{Z\Big(1+\frac{\delta_{l,0}}{n^3}\Big)}\,, \tag{28}$$

where $G_{\rm 2elQED}^{(7+)}$ is defined by Eq. (23), $E_{\rm 1loop,H}^{(7+)}$ is the one-loop part of $E_{\rm rad,H}^{(7+)}$, and c_1 is the $1/Z^1$ coefficient of the expansion of the matrix element of the δ function, see Eq. (25). The subtraction in Eq. (28) is needed in order to remove the double counting of terms already included into the approximation of Eq. (27).

In Table VI we collect our final results for the higher-order QED correction. For transparency, we separate the correction into three parts according to the order in $1/Z$ (the zeroth-, first-, and higher-order contributions). The $1/Z^0$ part is the one-electron contribution and is given by the sum $E_D^{(7+)}(nl_j) + E_{\rm rad,H}^{(7+)}(nl_j)$, as tabulated in Refs. [39, 42]. The $1/Z^1$ term consists of the one-photon exchange correction $E_{\rm 1ph}^{(7+)}$, the one-loop two-electron QED contribution $G_{\rm 2elQED}^{(7+)}$, and the two-loop two-electron QED contribution evaluated within the hydrogenic approximation. The $1/Z^{2+}$ term is given by the $1/Z^{2+}$ part of Eq. (27).

An important point is the estimation of the uncertainty of the higher-order QED correction, because it directly translates into the uncertainty of the total theoretical energies. The dominant error comes from the $1/Z^2$ one-loop QED effects. We estimate it by rescaling the corresponding $1/Z$ correction, with a conservative factor of 1.5,

$$1.5\,E_{\rm add}^{(7+)}\,\frac{c_2}{Zc_1}\,,$$

where c_1 and c_2 are the δ-function expansion coefficients from Eq. (25). Another uncertainty comes from the two-electon two-loop QED effects. It is important that to the order $m\alpha^7$, the hydrogenic approximation is exact for the two-loop effects [16], so that the uncertainty comes from the $m\alpha^{8+}$ contributions only. We take it to be 100% of the $1/Z\ m\alpha^{8+}$ two-loop QED correction, as delivered by the hydrogenic approximation. Furthermore, we include the uncertainty due to our extrapolation of $E_{\rm add}^{(7+)}$ (for $Z < 10$) and the uncertainty from the one-electron two-loop QED corrections [39, 42]. Adding all four uncertainties quadratically, we arrive at the error estimates listed in Table VI.

Table VI presents also results for the finite nuclear size (fns) correction. Although its nominal order is $m\alpha^4$, this correction is additionally suppressed by a square of the nuclear charge radius, which makes it comparable in magnitude to the $m\alpha^{7+}$ QED effects. Data presented in Table VI show that our theoretical predictions are sensitive to nuclear effects, specifically, to the fns correction. Defining the sensitivity as the ratio of the theoretical uncertainty in Table VI to the fns correction, we find that the best sensitivity is achieved for the $2\,^3S$ ionization energy, where it varies from 4% for $Z = 6$ till 1% for $Z = 30$.

VII. HIGHER-ORDER QED: MIXING STATES

Among the $n = 2$ states of He-like ions there are two that have the same values of the total angular momentum and parity, namely, the $2\,^1P_1$ and $2\,^3P_1$ states. These states strongly mix with each other, especially for medium-Z ions, and thus should be treated as quasidegenerate.

The QED theory of quasidegenerate states was developed in the framework of the two-time Green function approach in Refs. [8, 35]. Within this method, the energies of the $2\,^1P_1$ and $2\,^3P_1$ states are determined as eigenvalues of the effective 2×2 Hamiltonian in the jj coupling,

$$H^{jj} = \begin{pmatrix} \langle (1s2p_{1/2})_1|H|(1s2p_{1/2})_1\rangle & \langle (1s2p_{1/2})_1|H|(1s2p_{3/2})_1\rangle \\ \langle (1s2p_{3/2})_1|H|(1s2p_{1/2})_1\rangle & \langle (1s2p_{3/2})_1|H|(1s2p_{3/2})_1\rangle \end{pmatrix} \equiv \begin{pmatrix} H_{1/2} & H_{1/2,3/2} \\ H_{3/2,1/2} & H_{3/2} \end{pmatrix}, \tag{29}$$

with $H_{3/2,1/2} = H_{1/2,3/2}$. The all-order calculations described in Secs. III-V provide results for the matrix elements of the Hamiltonian H^{jj}.

For light ions, the LS-coupling scheme yield better results and the $Z\alpha$-expansion calculations are usually performed within the LS-coupling. For comparing with the $Z\alpha$-expansion calculations, it is convenient to transform the effective Hamiltonian H^{jj} delivered by the all-order calculations to the LS-coupling by [43]

$$H^{LS} = \mathcal{R}\, H^{jj}\, \mathcal{R}^{-1} \equiv \begin{pmatrix} H_T & H_{ST} \\ H_{ST} & H_S \end{pmatrix}, \tag{30}$$

where the unitary matrix $\mathcal{R}$ is

$$\mathcal{R} = \begin{pmatrix} a & -b \\ b & a \end{pmatrix}, \tag{31}$$

with $a = \sqrt{2/3}$ and $b = \sqrt{1/3}$. The indices S and T in the matrix elements stand for the singlet ($2\,^1P$) and triplet ($2\,^3P$) states, respectively. The explicit form of the matrix elements is

$$H_T = b^2\, H_{3/2} + a^2\, H_{1/2} - 2ab\, H_{1/2,3/2}\,, \tag{32}$$

$$H_S = a^2\, H_{3/2} + b^2\, H_{1/2} + 2ab\, H_{1/2,3/2}\,, \tag{33}$$

$$H_{ST} = ab\left[H_{1/2} - H_{3/2}\right] + \left(a^2 - b^2\right) H_{1/2,3/2}\,. \tag{34}$$

We note that the eigenvalues of H^{jj} and H^{LS} are the same since $\mathcal{R}$ is unitary.

The eigenvalues of H^{LS} denoted as E_S and E_T are obtained as

$$E_T = H_T + E_{\rm mix}\,, \tag{35}$$

$$E_S = H_S - E_{\rm mix}\,, \tag{36}$$

where $E_{\rm mix}$ is the mixing correction

$$E_{\rm mix} = \frac{H_T - H_S}{2}\left[\sqrt{1 + \left(\frac{2H_{ST}}{H_T - H_S}\right)^2} - 1\right]. \tag{37}$$

For small Z, the nondiagonal matrix element H_{ST} is suppressed by a factor of α^2 as compared to the diagonal ones. For this reason $E_{\rm mix}$ is a small correction when $Z \to 0$. For $|H_{ST}| \ll |H_S - H_T|$ we can expand the square root in Eq. (37), obtaining

$$E_{\rm mix} = \frac{H_{ST}^2}{H_T - H_S} + \frac{H_{ST}^4}{(H_T - H_S)^3} + \ldots. \tag{38}$$

The terms in the right-hand-side of this formula can be identified as the second-order, fourth-order, etc perturbation corrections for the single-level perturbation theory. This shows the equivalence of the perturbation theory for quasidegenerate states and that for a single level: the perturbation expansion for quasidegenerate states corresponds to a resummation of the expansion for the single level, accounting for terms with small energy denominators to all orders.

In Ref. [14], the mixing contribution was accounted for within the lowest order of perturbation theory (as a part of the $m\alpha^6$ correction),

$$E^{(6)}_{\rm mix} = \frac{\left[H^{(4)}_{ST}\right]^2}{H^{(2)}_T - H^{(2)}_S}\,, \tag{39}$$

where $H^{(2)}_T = E_0(2\,^3P)$ and $H^{(2)}_S = E_0(2\,^1P)$ are the nonrelativistic energies of the $2\,^3P$ and $2\,^1P$ states, respectively, and

$$H^{(4)}_{ST} = \langle 2\,^3P|H^{(4)}|2\,^1P\rangle\,, \tag{40}$$

with $H^{(4)}$ being the Breit Hamiltonian. In the present work, we extend this formula for $E_{\rm mix}$ by including higher-order corrections. Specifically, we take H_S and H_T to be the complete energies of the $2\,^1P$ and $2\,^3P$ states as evaluated in Ref. [14] (but without the mixing $m\alpha^6$ contribution) and the nondiagonal matrix element determined as

$$H_{ST} = H^{(4)}_{ST} + \alpha\, H^{(5)}_{ST} + \alpha^2\, H^{(6+)}_{ST}\,. \tag{41}$$

The $m\alpha^5$ correction to the nondiagonal matrix element is

$$H^{(5)}_{ST} = \langle 2\,^3P|H^{(5)}|2\,^1P\rangle\,, \tag{42}$$

where $H^{(5)}$ is the anomalous magnetic moment correction to the Breit Hamiltonian, given by Eq. (14) of Ref. [14]. Furthermore, $H^{(6+)}_{ST}$ is the correction to the nondiagonal matrix element of order $m\alpha^6$ and higher. In it we retain only the contribution of zeroth order in $1/Z$, which is, according to Eq. (34),

$$H^{(6+)}_{ST} = ab\left[E^{(6+)}_{\rm rad,H}(2p_{1/2}) - E^{(6+)}_{\rm rad,H}(2p_{3/2})\right], \tag{43}$$

where $E^{(6+)}_{\rm rad,H}(nl_j)$ is the one-electron radiative correction of order $m\alpha^6$ and higher.

Fig. 2 shows a comparison of the mixing correction $E_{\rm mix}$ evaluated within the $Z\alpha$-expansion approach in the LS coupling and the corresponding correction obtained with the all-order approach in the jj coupling (after the coupling transformation according to Eq. (30)). We find good agreement of the results obtained with different approaches. It is clearly seen that the leading-order formula (39) is adequate for very low Z but starts to deviate significantly from the complete results for $Z > 10$.

A detailed comparison between the all-order and $Z\alpha$-expansion calculations for the mixing states is complicated by the fact that the matrix elements of the effective Hamiltonian in different methods are not directly comparable to each other. It is known [44] that the effective Hamiltonian is defined up to a unitary transformation and the equivalence of different methods is achieved for the eigenvalues but not for individual matrix elements. More exactly, the equivalence of the matrix elements exists in the nonrelativistic limit but breaks down on the level of relativistic corrections. Indeed, we find perfect agreement for the leading coefficient of the $Z\alpha$ expansion of the two-photon exchange correction a_{20} as obtained from the NRQED calculation (see Table IV) and from the all-order calculations (after transformation to the LS coupling with Eq. (30)). Already for the next-order coefficient a_{40}, however, there is no direct equivalence on the level of individual matrix elements.

While a direct comparison of matrix elements in different methods does not seem to be possible, one can still [44] compare the *trace* of the Hamiltonian matrix since it is preserved by a unitary transformation. Indeed, we find that the sum of the a_{40} coefficients obtained from the all-order calculation for the $(1s2p_{1/2})_1$ and $(1s2p_{3/2})_1$ diagonal matrix elements yields $-0.252\,72$, which is close to $-0.252\,762$ obtained for the sum of the a_{40} coefficients for the $2\,^1P_1$ and $2\,^3P_1$ diagonal matrix elements in Table IV.

In Fig. 3 we present a comparison of the two-electron QED contribution for the sum of the diagonal $(1s2p_{1/2})_1$ and $(1s2p_{3/2})_1$ matrix elements evaluated with the all-order approach and within the $Z\alpha$-expansion method. The $Z\alpha$-expansion coefficients are taken from Tables IV and V. We observe that the all-order results converge to predictions of the $Z\alpha$ expansion in the low-Z region and that the difference is consistent with the expected magnitude of higher-order effects.

Despite good agreement between the two methods, we presently do not see a way to separate out the higher-order two-electron QED contribution that can be unambiguously added to $Z\alpha$-expansion results for the mixing states. The reason is that $E_{\rm mix}$ mixes different orders of $Z\alpha$ and $1/Z$ expansions so that some double-counting seems to be unavoidable. For this reason we restrict ourselves to retaining only the one-electron part of the higher-order QED effects. Our final results for the higher-order QED correction for the mixing states are summarized in Table VII. The $1/Z^0$ term is the sum of the Dirac energy and the radiative contribution. The radiative part is, according to Eqs. (32) and (33),

$$E^{(7+)}_{\rm rad,H}(2\,^3P_1) = \frac{1}{3}\,E^{(7+)}_{\rm rad,H}(2p_{3/2}) + \frac{2}{3}\,E^{(7+)}_{\rm rad,H}(2p_{1/2})\,, \tag{44}$$

$$E^{(7+)}_{\rm rad,H}(2\,^1P_1) = \frac{2}{3}\,E^{(7+)}_{\rm rad,H}(2p_{3/2}) + \frac{1}{3}\,E^{(7+)}_{\rm rad,H}(2p_{1/2})\,, \tag{45}$$

and the same for the Dirac energy $E^{(7+)}_D$. The $1/Z^{1+}$ term contains the radiative correction within the hydrogenic approximation (27). The fourth column shows results for the higher-order mixing correction $\delta E = E_{\rm mix} - E^{(6)}_{\rm mix}$. The finite nuclear size correction is listed in the fifth column of the table.

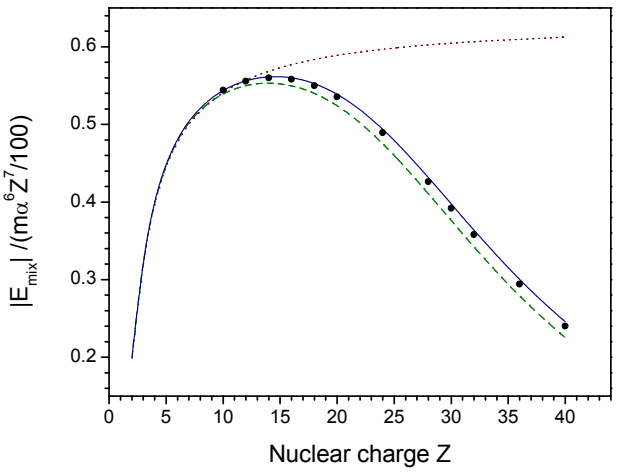

FIG. 2. The absolute value of the mixing correction $E_{\rm mix}$ divided by $m\alpha^6Z^7 \times 10^{-2}$. Black dots show results of all-order QED calculations, the dotted line (brown) is the contribution of the leading term of the α expansion $E^{(6)}_{\rm mix}$; the dashed line (green) corresponds to the complete formula (37) that includes the next-to-leading terms of the α expansion; the solid line (blue) is obtained with the complete formula including all known contributions, see text.

The dominant theoretical uncertainty is caused by the mixing correction. It comes through $H^{(6+)}_{ST}$ and is induced by contributions of order $1/Z^1$ and higher omitted in Eq. (43). We estimate the magnitude of the omitted effects as $(8/Z)\,H^{(6+)}_{ST}$, where the prefactor of $8 = n^3$ accounts for the fact that the $1/Z^1$ contribution is enhanced by the admixture of the $1s$ electron state.

The results collected in Table VII show that the higher-order mixing correction grows fast with increase of Z and becomes dominant already at $Z = 14$. Correspondingly, the uncertainty due to missing $1/Z^{1+}$ contributions in the non-diagonal matrix element $H^{(6+)}_{ST}$ becomes overwhelming for $Z > 14$. This reflects the failure of the LS coupling scheme and the advantage of using the jj coupling for medium and high-Z ions.

VIII. RESULTS AND DISCUSSION

In Table VIII we collect our final results for theoretical ionization energies of the ground and the non-mixing $n = 2$ excited states of helium-like ions with the nuclear charges $Z = 5-30$. We do not present results for $Z < 5$ since in this region the $1/Z$ expansion employed in the all-order approach ceases to be useful. For each element, calculations are performed for one isotope with the mass number A specified in the table. The nuclear masses are obtained from the atomic masses tabulated in Ref. [45] and the nuclear radii are taken from Ref. [46]. Our results include all non-recoil QED effects

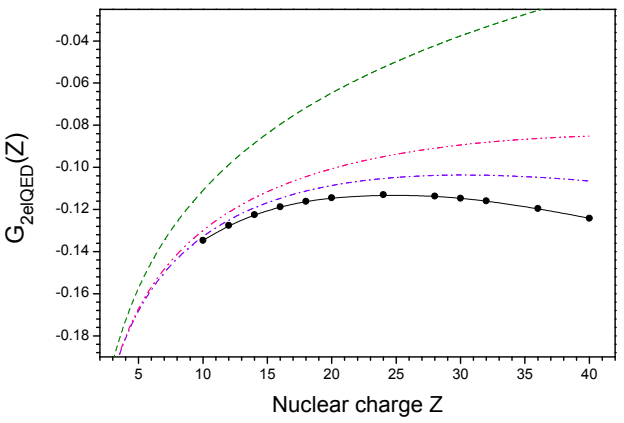

FIG. 3. The two-electron QED contribution for the sum of the diagonal $(1s2p_{1/2})_1$ and $(1s2p_{3/2})_1$ matrix elements, expressed in terms of the function $G_{\rm 2elQED}(Z)$ defined by Eq. (21). The line description is the same as for Fig. 1.

TABLE VII. The higher-order QED and finite nuclear size contributions for the mixing $n = 2$ states. Units are $m\alpha^2(Z\alpha)^5$.

Z	$1/Z^0$	$1/Z^{1+}$	MIX	FNS	Total
$2\,^1P_1$					
6	0.459	−0.149	0.174	0.027	0.51 (21)
8	0.539	−0.143	0.315	0.021	0.73 (30)
10	0.600	−0.131	0.311	0.019	0.80 (50)
14	0.671	−0.103	−1.930	0.012	−1.3 (13)
18	0.675	−0.071	−13.743	0.010	−13.1 (25)
20	0.649	−0.054	−27.391	0.009	−26.8 (33)
24	0.536	−0.017	−81.309	0.008	−80.8 (50)
28	0.333	0.023	−183.583	0.008	−183.2 (65)
30	0.193	0.045	−255.344	0.009	−255.1 (71)
$2\,^3P_1$					
6	0.537	0.742	−0.174	−0.129	0.98 (71)
8	0.623	0.703	−0.315	−0.094	0.92 (66)
10	0.681	0.667	−0.311	−0.079	0.96 (73)
14	0.718	0.619	1.930	−0.046	3.2 (14)
18	0.638	0.602	13.743	−0.035	14.9 (25)
20	0.549	0.603	27.391	−0.029	28.5 (33)
24	0.260	0.621	81.309	−0.022	82.2 (50)
28	−0.199	0.660	183.583	−0.017	184.0 (65)
30	−0.502	0.686	255.344	−0.016	255.5 (71)

up to order $m\alpha^6$ and the recoil effects up to order $m^2\alpha^5/M$, as calculated for $Z \leq 12$ in Ref. [14]. For $Z > 12$, we sum up the $1/Z$-expansion coefficients listed in Ref. [14]. In addition to the NRQED results, we include the higher-order $m\alpha^{7+}$ correction calculated in this work and summarized in Table VI.

In Table VIII our present results are compared with those from our previous work [14] and by other authors [8–10]. For $Z \geq 12$, our calculation is in excellent agreement with previous calculations performed within the all-order approach [8–10] and improves their accuracy by more than an order of magnitude. For $Z \leq 12$, we significantly improve upon our previous results [14] but also find small deviations in some cases. The reason for the deviations is that the hydrogenic approximation used in Ref. [14] for estimations of the higher-order two-electron QED effects turned out to be less accurate than expected. Indeed, it can be seen from Figs. 1 and 2 that the addition of the higher-order correction calculated within the hydrogenic approximation leads to significant improvements only in the case of the $2\,^3S$ state. For other states, the hydrogenic approximation largely overestimates the actual contribution and even worsens the results for the $2\,^1P_0$ and $2\,P_1$ states. We conclude that in the case under consideration the hydrogenic approximation yields only the order of magnitude of the effect but does not provide a quantitative prediction.

In Table IX we present theoretical energies for the mixing states, $2\,^1P_1$ and $2\,^3P_1$. As compared to our previous investigation [14], we added the higher-order mixing correction and re-evaluated the uncertainty. The values of theoretical energies did not change much, but the uncertainty was increased typically by a factor of 2 or 3. Our results for $Z = 12$ are in good agreement with the values by Artemyev *et al.* [8]. We do not report results for $Z > 12$ for the mixing states, since their uncertainty increases rapidly (see Table VII) and the present method becomes less accurate than all-order calculations in the jj coupling [8–10].

Table X compares our theoretical predictions for the intrashell $n = 2$ transition energies in helium-like ions with results of previous calculations and available experimental data. We observe that for transitions between non-mixing states, our calculation improves the theoretical accuracy typically by an order of magnitude as compared to the previous calculations. Theoretical and experimental results summarized in the table are in good agreement with each other. The differences are consistent with the combined error estimates and are of different signs, which leads to the conclusion that no systematic deviation is observed. The differences grow rapidly with Z, which reflects the fact that both theoretical and experimental uncertainties are strongly Z-dependent. The theoretical predictions for transitions between non-mixing states are more accurate than the experimental results for the whole interval of Z studied. By contrast, for transitions involving the mixing states the theoretical accuracy is significantly lower. Results for the fine-structure intervals are presented for the sake of completeness since more accurate calculations with full inclusion of the $m\alpha^7$ effects are available in this case [12].

Summarizing, we performed a high-precision calculation of the two-electron QED effects to all orders in the nuclear binding strength parameter $Z\alpha$ and identified the higher-order QED effects of order $m\alpha^7$ and higher. By using the "unified" approach, we combined together the NRQED calculation of Ref. [14] complete to order $m\alpha^6$ and all-order calculations of one-electron and two-electron QED effects. In the result we obtained improved theoretical predictions for ionization energies of the ground and non-mixing $n = 2$ states of helium-like ions with $Z = 5-30$. Theoretical predictions for the mixing $2\,^1P_1$ and $2\,^3P_1$ states are obtained for $Z = 5-12$. Their accuracy is lower than that for the non-mixing states since the higher-order QED effects are included within the one-electron approximation only. In order to advance the theory of the mixing states further, one needs to extend the NRQED approach

to embrace the perturbation theory of quasidegenerate states.

ACKNOWLEDGMENTS

The authors are grateful to A. N. Artemyev for participation at the earlier stages of the calculations and to A. V. Malyshev for useful discussions. The work was supported by the Russian Science Foundation (Grant No. 20-62-46006). K.P. acknowledges support from the National Science Center (Poland) Grant No. 2017/27/B/ST2/02459. Computations were performed partly in the computer cluster "Tornado" of St. Petersburg Polytechnic University.

[1] G. W. F. Drake, editor, *Handbook of Atomic, Molecular, and Optical Physics*, Springer, Berlin, 2005.
[2] G. W. F. Drake, Review oh high precision theory and experiment for helium, in *The Hydrogen Atom. Precision Physics of Simple Atomic Systems*, edited by S. G. Karshenboim, F. S. Pavone, G. F. Bassani, M. Inguscio, and T. W. Hänsch, Lecture Notes in Physics, pages 57 – 80, Berlin, 2001, Springer.
[3] G. Drake and Z.-C. Yan, Can. J. Phys. **86**, 45 (2008).
[4] P. Indelicato, J. Phys. B **52**, 232001 (2019).
[5] H. Persson, S. Salomonson, P. Sunnergren, and I. Lindgren, Phys. Rev. Lett. **76**, 204 (1996).
[6] A. N. Artemyev, V. M. Shabaev, and V. A. Yerokhin, Phys. Rev. A **56**, 3529 (1997).
[7] V. A. Yerokhin, A. N. Artemyev, and V. M. Shabaev, Phys. Lett. A **234**, 361 (1997).
[8] A. N. Artemyev, V. M. Shabaev, V. A. Yerokhin, G. Plunien, and G. Soff, Phys. Rev. A **71**, 062104 (2005).
[9] Y. S. Kozhedub, A. V. Malyshev, D. A. Glazov, V. M. Shabaev, and I. I. Tupitsyn, Phys. Rev. A **100**, 062506 (2019).
[10] A. V. Malyshev, Y. S. Kozhedub, D. A. Glazov, I. I. Tupitsyn, and V. M. Shabaev, Phys. Rev. A **99**, 010501 (2019).
[11] K. Pachucki, V. Patkóš, and V. A. Yerokhin, Phys. Rev. A **95**, 062510 (2017).
[12] K. Pachucki and V. A. Yerokhin, Phys. Rev. Lett. **104**, 070403 (2010).
[13] G. W. F. Drake, Can. J. Phys. **66**, 586 (1988).
[14] V. A. Yerokhin and K. Pachucki, Phys. Rev. A **81**, 022507 (2010).
[15] V. A. Yerokhin, M. Puchalski, and K. Pachucki, Phys. Rev. A **102**, 042816 (2020).
[16] V. Patkóš, V. A. Yerokhin, and K. Pachucki, Phys. Rev. A **103**, 042809 (2021).
[17] G. Clausen, P. Jansen, S. Scheidegger, J. A. Agner, H. Schmutz, and F. Merkt, Phys. Rev. Lett. **127**, 093001 (2021).
[18] V. A. Yerokhin, V. Patkóš, and K. Pachucki, Phys. Rev. A **98**, 032503 (2018), *ibid.* **103**, 029901(E) (2021).
[19] V. Patkóš, V. A. Yerokhin, and K. Pachucki, Phys. Rev. A **101**, 062516 (2020), *ibid.* **103**, 029902(E) (2021).
[20] V. A. Yerokhin and A. V. Maiorova, Symmetry **12**, 800 (2020).
[21] V. A. Yerokhin and V. M. Shabaev, Phys. Rev. A **60**, 800 (1999).
[22] V. A. Yerokhin, K. Pachucki, and V. M. Shabaev, Phys. Rev. A **72**, 042502 (2005).
[23] V. A. Yerokhin, A. N. Artemyev, T. Beier, G. Plunien, V. M. Shabaev, and G. Soff, Phys. Rev. A **60**, 3522 (1999).
[24] V. A. Yerokhin, K. Pachucki, M. Puchalski, C. H. Keitel, and Z. Harman, Phys. Rev. A **102**, 022815 (2020).
[25] A. G. Fainshtein, N. L. Manakov, and A. A. Nekipelov, J. Phys. B **24**, 559 (1991).
[26] N. L. Manakov and A. A. Nekipelov, Vestnik Voronezhskogo gosudarstvennogo universiteta **2**, 53 (2012), [in Russian, http://www.vestnik.vsu.ru/pdf/physmath/2012/02/2012-02-07.pdf].
[27] N. L. Manakov and A. A. Nekipelov, Vestnik VGU **2**, 84 (2013), [in Russian, http://www.vestnik.vsu.ru/pdf/physmath/2013/02/2013-02-08.pdf].
[28] W. R. Johnson, S. A. Blundell, and J. Sapirstein, Phys. Rev. A **37**, 307 (1988).
[29] A. N. Artemyev, Private communication, 2020.
[30] S. A. Blundell, P. J. Mohr, W. R. Johnson, and J. Sapirstein, Phys. Rev. A **48**, 2615 (1993).
[31] P. J. Mohr and J. Sapirstein, Phys. Rev. A **62**, 052501 (2000).
[32] O. Y. Andreev, L. N. Labzowsky, G. Plunien, and G. Soff, Phys. Rev. A **64**, 042513 (2001).
[33] B. Åsen, S. Salomonson, and I. Lindgren, Phys. Rev. A **65**, 032516 (2002).
[34] O. Y. Andreev, L. N. Labzowsky, G. Plunien, and G. Soff, Phys. Rev. A **69**, 062505 (2004).
[35] V. M. Shabaev, Phys. Rep. **356**, 119 (2002).
[36] I. Lindgren, H. Persson, S. Salomonson, and L. Labzowsky, Phys. Rev. A **51**, 1167 (1995).
[37] V. M. Shabaev, I. I. Tupitsyn, V. A. Yerokhin, G. Plunien, and G. Soff, Phys. Rev. Lett. **93**, 130405 (2004).
[38] V. A. Yerokhin, C. H. Keitel, and Z. Harman, Phys. Rev. A **104**, 022814 (2021).
[39] V. A. Yerokhin, K. Pachucki, and V. Patkóš, Ann. Phys. (Leipzig) **531**, 1800324 (2019).
[40] S. G. Karshenboim, Z. Phys. D **39**, 109 (1997).
[41] P. J. Mohr, Phys. Rev. Lett. **34**, 1050 (1975).
[42] V. A. Yerokhin and V. M. Shabaev, J. Phys. Chem. Ref. Data **44**, 033103 (2015).
[43] G. W. F. Drake, Nucl. Instrum. Methods **B 202**, 273 (1982).
[44] A. Malyshev, Y. Kozhedub, I. Anisimova, D. Glazov, M. Kaygorodov, I. Tupitsyn, and V. Shabaev, Optics and Spectroscopy **129**, 652 (2021).
[45] M. Wang, G. Audi, A. H. Wapstra, F. G. Kondev, M. MacCormick, X. Xu, and B. Pfeiffer, Chin. Phys. C **36**, 1603 (2012).
[46] I. Angeli and K. Marinova, At. Dat. Nucl. Dat. Tabl. **99**, 69 (2013).
[47] T. P. Dinneen, N. Berrah-Mansour, H. G. Berry, L. Young, and R. C. Pardo, Phys. Rev. Lett. **66**, 2859 (1991).
[48] N. J. Peacock, M. F. Stamp, and J. D. Silver, Phys. Scr. **T8**, 10 (1984).
[49] W. Curdt, E. Landi, K. Wilhelm, and U. Feldman, Phys. Rev. A **62**, 022502 (2000).
[50] K. W. Kukla, A. E. Livingston, J. Suleiman, H. G. Berry, R. W. Dunford, D. S. Gemmell, E. P. Kanter, S. Cheng, and L. J. Curtis, Phys. Rev. A **51**, 1905 (1995).
[51] J. P. Buchet, M. C. Buchet-Poulizac, A. Denis, J. Désesquelles, M. Druetta, J. P. Grandin, and X. Husson, Phys. Rev. A **23**, 3354 (1981).
[52] H. A. Klein, F. Moscatelli, E. G. Myers, E. H. Pinnington, J. D. Silver, and E. Trabert, J. Phys. B **18**, 1483 (1985).
[53] J. K. Thompson, D. J. H. Howie, and E. G. Myers, Phys. Rev.

TABLE VIII. Theoretical ionization energies of the ground and the non-mixing $n = 2$ excited states of helium-like ions, in eV, $1\,\mathrm{eV} = 27.211\,386\,245\,988$ a.u.

Z	A	$1\,^1S_0$	$2\,^1S_0$	$2\,^3S_1$	$2\,^3P_0$	$2\,^3P_2$	Ref.
5	11	259.374 4095 (15)	56.569 281 05 (80)	60.806 181 969 (85)	56.417 932 23 (60)	56.413 410 95 (26)	
		259.374 40 (2)	56.569 277 (15)	60.806 181 (17)	56.417 930 9 (5)	56.413 410 4 (4)	[14]
6	12	392.090 5875 (26)	87.702 7960 (14)	93.128 352 06 (18)	87.685 5982 (11)	87.670 310 62 (50)	
7	14	552.067 4680 (43)	125.652 8520 (24)	132.275 521 40 (34)	125.776 2109 (20)	125.739 052 56 (88)	
8	16	739.327 0757 (67)	170.427 3032 (39)	178.254 625 55 (62)	170.694 2194 (33)	170.618 5383 (15)	
9	19	953.898 447 (10)	222.035 5951 (59)	231.075 0281 (11)	222.446 8404 (50)	222.309 3293 (23)	
10	20	1195.808 475 (15)	280.486 8810 (86)	290.746 1290 (17)	281.042 6591 (74)	280.812 2429 (34)	
11	23	1465.099 543 (22)	345.794 144 (12)	357.281 4596 (27)	346.492 900 (11)	346.129 6103 (49)	
12	24	1761.805 457 (29)	417.968 719 (16)	430.692 9183 (30)	418.809 227 (14)	418.263 0745 (64)	
		1761.804 9 (10)	417.968 56 (11)	430.692 90 (11)	418.809 14 (2)	418.263 03 (2)	[14]
		1761.804 7 (2)	417.968 9 (1)	430.692 9 (1)	418.809 2 (1)	418.263 0 (1)	[8]
13	27	2085.977 675 (39)	497.026 358 (21)	510.996 9945 (43)	498.005 959 (18)	497.215 7863 (86)	
14	28	2437.658 788 (51)	582.981 104 (26)	598.208 4225 (55)	584.097 729 (23)	582.990 066 (11)	
15	31	2816.909 423 (63)	675.851 568 (33)	692.346 6318 (70)	677.101 841 (30)	675.589 728 (14)	
16	32	3223.781 337 (80)	775.654 618 (41)	793.429 2528 (89)	777.035 871 (37)	775.017 688 (17)	
17	35	3658.344 41 (10)	882.411 785 (51)	901.478 679 (12)	883.920 107 (46)	881.278 372 (22)	
18	40	4120.666 36 (13)	996.144 406 (62)	1016.517 087 (15)	997.775 684 (57)	994.375 840 (26)	
		4120.667 2 (9)	996.144 3 (3)	1016.516 8 (2)	997.775 4 (2)	994.375 6 (2)	[10]
		4120.665 3 (4)	996.144 6 (2)	1016.517 0 (1)	997.775 8 (3)	994.375 7 (1)	[8]
19	39	4610.807 89 (16)	1116.872 475 (75)	1138.565 273 (19)	1118.624 164 (69)	1114.313 372 (32)	
20	40	5128.858 40 (19)	1244.623 304 (89)	1267.651 485 (24)	1246.490 895 (82)	1241.096 747 (38)	
21	45	5674.904 20 (23)	1379.423 80 (11)	1403.803 533 (30)	1381.402 010 (98)	1374.731 277 (45)	
22	48	6249.023 07 (28)	1521.299 10 (12)	1547.047 425 (37)	1523.383 92 (12)	1515.221 274 (53)	
23	51	6851.311 46 (34)	1670.279 22 (15)	1697.414 119 (45)	1672.465 89 (14)	1662.572 575 (62)	
24	52	7481.863 27 (41)	1826.394 10 (17)	1854.934 471 (54)	1828.678 23 (16)	1816.790 721 (72)	
25	55	8140.787 72 (49)	1989.677 64 (20)	2019.643 353 (66)	1992.053 73 (18)	1977.882 359 (84)	
26	56	8828.188 09 (58)	2160.162 56 (23)	2191.574 459 (79)	2162.625 73 (21)	2145.853 312 (96)	
		8828.189 6 (25)	2160.162 5 (8)	2191.574 2 (7)	2162.625 3 (7)	2145.853 0 (7)	[9]
		8828.187 5 (11)	2160.163 2 (7)	2191.574 5 (6)	2162.626 1 (10)	2145.853 2 (2)	[8]
27	59	9544.183 39 (68)	2337.886 07 (26)	2370.765 981 (94)	2340.430 43 (24)	2320.710 82 (11)	
28	58	10288.886 21 (80)	2522.883 72 (29)	2557.254 48 (11)	2525.504 31 (28)	2502.460 95 (13)	
29	63	11062.431 11 (94)	2715.197 98 (34)	2751.083 47 (13)	2717.888 06 (32)	2691.112 45 (14)	
30	64	11864.939 4 (11)	2914.866 90 (38)	2952.292 00 (15)	2917.621 11 (36)	2886.671 37 (16)	

TABLE IX. Same as Table VIII but for the mixing $n = 2$ states.

Z	$2\,^1P_1$	$2\,^3P_1$	Ref.
5	53.809 194 15 (36)	56.419 9395 (14)	
	53.809 194 4 (1)	56.419 9393 (4)	[14]
6	84.188 092 04 (92)	87.687 1467 (31)	
7	121.371 7397 (23)	125.775 1315 (64)	
8	165.365 9011 (55)	170.686 923 (12)	
9	216.176 651 (13)	222.428 084 (22)	
10	273.807 646 (28)	281.005 369 (41)	
11	338.266 548 (59)	346.428 077 (75)	
12	409.556 49 (12)	418.705 94 (13)	
	409.556 460 (6)	418.705 96 (17)	[14]
	409.556 4 (1)	418.705 9 (1)	[8]

A **57**, 180 (1998).
[54] E. G. Myers and M. R. Tarbutt, Phys. Rev. A **61**, 010501 (1999).
[55] E. G. Myers, D. J. H. Howie, J. K. Thompson, and J. D. Silver, Phys. Rev. Lett. **76**, 4899 (1996).

TABLE X. Comparison of theoretical and experimental $n = 2$ intrashell transition energies, in cm^{-1}.

Z	Theory	Experiment	Difference	Ref.
$2\,^3S_1$–$2\,^3P_0$				
5	35 393.6211 (49)	35 393.627 (13)	−0.006 (13)	[47]
	35 393.628 (14)[a]			
8	60 978.788 (27)	60 978.44 (52)	0.35 (52)	[48]
	60 978.85 (14)[a]			
12	95 848.43 (11)	95 851.27 (92)	0.15 (93)	[49]
	95 849.0 (9)[a]			
	95 848.(1)[b]			
14	113 810.42 (19)	113 806.7 (3.7)	3.7 (3.7)	[49]
	113 809.(2)[b]			
18	151 159.61 (47)	151 164.0 (4.1)	−4.4 (4.1)	[50]
	151 158.(3)[b]			
26	233 487.3(1.8)	232 558. (550)	71.(550)	[13]
	233 484.(10)[b]			
	233 485.(9)[c]			
$2\,^3S_1$–$2\,^3P_2$				
5	35 430.0876 (22)	35 430.084 (9)	0.004 (9)	[47]
	35 430.088 (14)[a]			
7	52 720.1766 (76)	52 720.23 (69)	−0.05 (69)	[48]
	52 720.18 (7)[a]			
8	61 589.198 (13)	61 589.70 (53)	−0.50 (53)	[48]
	61 589.21 (14)[a]			
10	80 122.195 (31)	80 123.33 (83)	−1.1 (0.8)	[48]
	80 122.3 (4)[a]			
12	100 253.451 (57)	100 255.9 (1.9)	−2.5 (1.9)	[49]
	100 253.7 (9)[a]			
	100 253. (1)[b]			
14	122 744.326 (98)	122 740.4 (3.6)	3.9 (3.6)	[49]
	122 744.(1)[b]			
18	178 581.19 (24)	178 589.3 (5.1)	−8.1 (5.1)	[50]
	178 581.(2)[b]			
26	368 765.9(1.0)	368 976.(125)	−210.(125)	[51]
	368 767.(6)[b]			
	368 767.(5)[c]			
$2\,^3S_1$–$2\,^3P_1$				
5	35 377.432 (11)	35 377.424 (13)	0.008 (17)	[47]
	35 377.429 (14)[a]			
8	61 037.634 (99)	61 037.62 (93)	0.01 (93)	[48]
	61 037.65 (14)[a]			
12	966 81.5 (1.1)	966 83.(6)	−2. (6)	[52]
	966 82.(1)[a]			
$2\,^1S_0$–$2\,^3P_1$				
7	986.251 (55)	986.3180 (7)	−0.07 (6)	[53]
	986.36 (7)[a]			
$2\,^3P_0$–$2\,^3P_1$				
7	8.706 (54)	8.6707 (7)	0.035 (54)	[53]
	8.675 (21)[a]			
	8.6731 (67)[d]			
12	833.0 (1.1)	833.133 (15)	−0.1 (1.1)	[54]
	832.2 (0.2)[a]			
	834.(1)[b]			
$2\,^3P_2$–$2\,^3P_1$				
9	957.82 (18)	957.8730 (12)	−0.05 (18)	[55]
	957.797 (54)[a]			
	957.886 (79)[d]			

[a] Yerokhin and Pachucki 2010 [14]; [b] Artemyev *et al.* 2005 [8];
[c] Kozhedub *et al.* 2019 [9]; [d] Pachucki and Yerokhin 2010 [12].